J. CHEM. SOC. FARADAY TRANS., 1993, 89(12), 1915–1924

Temperature-independent Paramagnetism in Closed-shell Oxoanions of First-row Transition Metals

Patrick W. Fowler and Erich Steiner
Department of Chemistry, University of Exeter, Stocker Road, Exeter, UK EX4 4QD

A consistent picture of the magnetism of the series of isoelectronic molecules VO_4^{3-}, CrO_4^{2-} and MnO_4^- is given by coupled Hartree–Fock theory. An external magnetic field induces a paramagnetic circulation around each nucleus that decreases in strength and extent from MnO_4^- to VO_4^{3-}. The presence of low-lying empty orbitals derived from splitting of the partially occupied valence shell leads to a significant paramagnetic contribution to the total magnetizability. As the central charge falls, the bonding becomes more ionic, the metal–oxygen bond grows longer and the diamagnetic susceptibility increases in magnitude. At the same time, in Hartree–Fock theory, the virtual orbitals become more diffuse and the paramagnetic contribution falls: 160.7 au (1 au = $e^2a_0^2/m_e \approx 7.891\,04 \times 10^{-29}$ J T^{-2}) in MnO_4^-, which is about twice the estimated experimental value, 86.0 au in CrO_4^{2-}, which is 10% too high, and 80.8 au in VO_4^{3-} (no experimental value). As a result the anions change from 'strongly' paramagnetic to magnetically neutral; at the experimental bond lengths total magnetizabilities are 93.2 au in MnO_4^- (exp. 8.3), 13.6 au in CrO_4^{2-} (exp. 6.3) and −0.8 au in VO_4^{3-}. Lattice effects on the computed values are very small. Agreement with experiment is better at the SCF bond lengths. It is concluded that the Hartree–Fock model becomes more appropriate as the system becomes more ionic, and gives an accurate description of the magnetism in VO_4^{3-}.

1. Introduction

The temperature-dependent paramagnetism of transition-metal compounds arising from the presence of a permanent magnetic moment, and associated with unpaired electron spins or incomplete valence shells, is well known and has been the subject of much study. Less well known is that several compounds of the transition metals, which exist in closed-shell ground states and do not have a permanent magnetic moment, exhibit temperature-independent or Van Vleck paramagnetism.[1] In particular, several of the simple tetrahedral oxides XO_4^{n-} of transition metals in the formal d^0 configuration are known to be paramagnetic. The most widely quoted examples are the permanganate, MnO_4^-, and chromate, CrO_4^{2-}, ions. In a previous study,[2] accurate coupled Hartree–Fock calculations of the magnetizability of MnO_4^- have shown that this ion is paramagnetic in Hartree–Fock theory, but that the computed magnetizability is strongly dependent on bond length, and is too large by an order of magnitude at the experimental bond length (for the ion in $KMnO_4$). This incorrect behaviour is a manifestation of the known inability of Hartree–Fock theory to describe accurately the bonding in metal complexes, particularly when π-bonding is present.[3,4] There are reasons to believe however that the deficiencies of Hartree–Fock theory may be less severe for elements to the left and below manganese in the Periodic Table.

The stable species XO_4^{n-} that have been characterised in the solid state are the isoelectronic series VO_4^{3-}, CrO_4^{2-} and MnO_4^-; MoO_4^{2-}, TcO_4^- and RuO_4; WO_4^{2-}, ReO_4^- and OsO_4.[5] Of these, MnO_4^- and CrO_4^{2-} in the first series[6,7] and TcO_4^- [8] in the second series are known to be paramagnetic, whereas MoO_4^{2-},[9,10] WO_4^{2-},[9–11] ReO_4^- [8,12] and OsO_4 [13,14] are diamagnetic. In this paper we describe the computation of the magnetic properties of the anions of V, Cr and Mn, and of the unknown FeO_4, in the $^1A_1$ ground state within the coupled Hartree–Fock model in an accurate and uniform basis. It will be shown that the deficiencies of Hartree–Fock theory become less severe on going from Mn to Cr to V, with CrO_4^{2-} paramagnetic within the model and VO_4^{3-} having near-zero magnetizability. Model calculations for the ions in a point-charge lattice show that the lattice electrostatics can be expected to have little effect on the properties of the ions.

2. Experimental Structures and Properties

Orthovanadate

The structure of VO_4^{3-} in several ionic solids has been determined. The structure of $LaVO_4$ [15] is monoclinic with lattice parameters $a = 7.047$ Å, $b = 7.286$ Å, $c = 6.725$ Å and $\beta = 104.85°$, with four molecules per unit cell. The VO_4^{3-} unit is tetrahedral with bond lengths 1.709 ± 0.015 Å and mean value $\bar{R} = 1.709$ Å, and with angles $108.3 \pm 7.5°$ and mean value 109.5°. Other examples are VO_4^{3-} in YVO_4 [16] with $\bar{R} = 1.706$ Å and in $InVO_4$ [17] with $\bar{R} = 1.727$ Å. In the present work, the 'experimental geometry' is chosen to be regular tetrahedral with bond length 1.709 Å = $3.23a_0$, which is also the mean bond length for VO_4^{3-} quoted by Krebs and Hasse.[5]

No measurements of the magnetic susceptibility of VO_4^{3-} appear to have been made, but several other oxides of vanadium show temperature-independent paramagnetism;[7] V_2O_5 with molar susceptibility $\chi_m = 60 \times 10^{-6}$ cgs emu,† NH_4VO_3 with $\chi_m = 14 \times 10^{-6}$ cgs emu, and $NaVO_3$ with $\chi_m = 20 \times 10^{-6}$ cgs emu. Accurate self-consistent (SCF) calculation of susceptibilities gives $\chi_m(Na^+) = -5.1 \times 10^{-6}$ cgs emu and $\chi_m(NH_4^+) = -15.0 \times 10^{-6}$ cgs emu, leading to the values for the 'VO_3^-' unit of 25×10^{-6} and 29×10^{-6} cgs emu. No such isolated unit has been observed in solid or solution, and the derived susceptibilities refer to the polymeric species.

Chromate

The structure of CrO_4^{2-} in the alkali-metal chromates is very closely regular tetrahedral. Na_2CrO_4 [18] has an orthorhombic structure with lattice parameters $a = 5.862$ Å, $b = 9.291$ Å, $c = 7.145$ Å with four molecules per unit cell. The CrO_4^{2-} unit has bond lengths 1.645 ± 0.010 Å with $\bar{R} = 1.645$ Å, and angles $109.3 \pm 0.5°$ with mean value 109.2°. Similarly, the bond lengths in K_2CrO_4 [19] are 1.646 ± 0.008 Å and in Li_2CrO_4 [20] they are 1.652 ± 0.005 Å. In the 1 : 1 compound $HgCrO_4$ [21] the bond lengths are 1.658 ± 0.054 Å with mean value 1.658 Å, and bond angles $109.6 \pm 2.1°$ with mean value 109.5°. The model geometry used in this work is regular tetrahedral with bond length 1.645 Å = $3.11a_0$.

† 1 cgs emu = 10 J T^{-2} mol^{-1}.

Measurements of the magnetic susceptibility of a number of chromates show that the chromate ion is paramagnetic, with magnetizability $\xi \approx 6.3$ au, corresponding to molar susceptibility $\chi_m(CrO_4^{2-}) \approx 30 \times 10^{-6}$ cgs emu. For K_2CrO_4, published values of the molar susceptibility are +8,[22] 0.0 [23] and -4×10^{-6} cgs emu.[9] Subtracting the computed SCF susceptibility for the potassium ion [$\chi_m = -15.4 \times 10^{-6}$ cgs emu (ref. 2)] gives the values 39, 31 and 27×10^{-6} cgs emu for the molar susceptibility $\chi_m(CrO_4^{2-})$ of the chromate ion. For Na_2CrO_4, the values 19 [23] and 11×10^{-6} cgs emu[9] give 29 and 21×10^{-6} cgs emu for the ion. Similarly, the value $\chi_m(CrO_4^{2-}) = 31 \times 10^{-6}$ cgs emu is obtained from the molar susceptibility $1.0 \pm 0.38 \times 10^{-6}$ cgs emu of the ammonium salt.[24] The average value is $\chi_m(CrO_4^{2-}) = 30 \times 10^{-6}$ cgs emu, corresponding to magnetizability $\xi = 6.3$ au. Other measurements listed in the tabulations of Landolt and Börnstein[13] are mostly consistent with this value, which is taken as our estimated 'experimental' magnetizability of the chromate ion.

Permanganate

The experimental structure and properties of MnO_4^- have been discussed in our previous work.[2] MnO_4^- exists as a complex ion in $KMnO_4$,[25] which has an orthorhombic structure with lattice parameters $a = 9.105$ Å, $b = 5.720$ Å, $c = 7.425$ Å with four molecules per unit cell. The ion is closely regular tetrahedral with average bond length 1.620 Å $= 3.0784a_0$. Measurements of the magnetic susceptibility of $KMnO_4$ [6,7] give magnetizability $\xi(MnO_4^-) = 8.34$ au ($\chi_m = 39.6 \times 10^{-6}$ cgs emu).

3. Basis Sets

The basis sets for the metals used in the present work are given in the Appendix, and they form part of a set for the whole first-row transition series.[26] They were derived from Huzinaga's energy-optimized (14s9p5d) sets for the neutral atoms[27] by extension, contraction and polarization to (16s12p6d4f/9s7p3d2f) using a recipe based on earlier work by Sadlej.[28–30] The basis set for Mn is somewhat smaller than the largest basis used in our previous work,[2] but gives an almost identical value for the magnetizability.

The oxygen set (10s6p4d/10s6p2d) is Sadlej's polarized set (10s6p4d/5s3p2d),[28,29] but with the s and p functions decontracted. This is to minimize the spurious gauge dependence of the magnetizability.

4. Gauge Dependence of the Magnetizability

The total magnetizability tensor of a molecule in its ground state Ψ_0 is[31]

$$\xi_{\alpha\beta} = \xi^d_{\alpha\beta} + \xi^p_{\alpha\beta} \tag{1}$$

where the tensor components are

$$\xi^d_{\alpha\beta} = \frac{1}{4}\left\langle \Psi_0 \left| \sum_i (r_{i\alpha} r_{i\beta} - \delta_{\alpha\beta} r_i^2) \right| \Psi_0 \right\rangle \tag{2}$$

and

$$\xi^p_{\alpha\beta} = \sum_{n \neq 0} \frac{2\mathscr{R}\left\{ \left\langle \Psi_0 \left| \sum_i m_{i\alpha} \right| \Psi_n \right\rangle \left\langle \Psi_n \left| \sum_i m_{i\beta} \right| \Psi_0 \right\rangle \right\}}{(E_n - E_0)} \tag{3}$$

and where $\boldsymbol{r}_i$ is the position vector of the ith electron and $\boldsymbol{m}_i$ its magnetic moment,† both defined with respect to the same origin of vector potential. $\{\Psi_n, E_n\}$ is the complete set of eigenstates and energies, α, β are cartesian directions and all quantities are expressed in atomic units. For a regular tetrahedral molecule both tensors are isotropic with diagonal components $\xi^d < 0$ and $\xi^p > 0$.

In the orbital approximation, the diamagnetizability is the sum of orbital contributions:

$$\xi^d = \xi^d_{\alpha\alpha} = -\frac{1}{6}\left\langle \Psi_0 \left| \sum_i r_i^2 \right| \Psi_0 \right\rangle = \sum_n \xi^d_n \tag{4}$$

where

$$\xi^d_n = -\tfrac{1}{3}\langle \psi_n | r^2 | \psi_n \rangle \tag{5}$$

is the contribution of the (doubly occupied) orbital ψ_n. ξ^d is essentially the moment of inertia of the electron distribution with respect to the origin of coordinates, and has minimum magnitude when the origin is at the electronic centroid.[32]

The violation of gauge invariance for our molecular anions arises mainly from deficiencies in the description of the oxygen charge clouds displaced from the centroid. For a closed-shell atom ($R = 0$ for the atom at the origin):

(*a*) The total diamagnetizability is

$$\xi^d(R) = \xi^d(0) - NR^2/6$$

where N is the number of electrons, and for each doubly occupied orbital,

$$\xi^d_n(R) = \xi^d_n(0) - R^2/3$$

This dependence on displacement R is independent of the basis.

(*b*) The exact total paramagnetizability is

$$\xi^p(R) = aR^2 = NR^2/6$$

but the orbital contributions depend on the system, because the loss of spherical symmetry about the origin leads to a mixing of orbitals with different angular momenta. For each orbital

$$\xi^p_n(R) = a_n R^2$$

where a_n depends on the system. The actual behaviour of the computed quantities is that both a and a_n depend on the system and on the basis.

When contracted basis sets are used, however large, the gauge-dependence error comes almost wholly from inflexible description of atomic inner shells. For the tetrahedral oxides of interest here, the relevant oxygen orbitals are 1s and 2s. Studies of the behaviour of the O^{2-} ion (similar results are obtained for other atoms) show that the error (under-estimate) in ξ^p is $\Delta\xi^p \approx 0.34R^2$ for the contracted Sadlej set,[28,29] or $1.36R^2$ for the four oxygens in XO_4^{n-}, and that this is reduced to $\Delta\xi^p \approx 0.018R^2$ for the uncontracted basis used in the present work, or $0.072R^2$ for the four oxygens. With a typical bond length of *ca.* $3a_0$, the systematic gauge-dependence error in the results presented in this paper is therefore *ca.* 0.7 au.

5. Calculations for the Free Ions

Second-order magnetic properties were calculated for the free ions in T_d symmetry at the model bond lengths $3.23a_0$ for VO_4^{3-}, $3.11a_0$ for CrO_4^{2-} and $3.0784a_0$ for MnO_4^-. All the calculations used the Exeter version of the Modena SYSMO program.[33] The computed properties are listed in Tables 1 (energies and Mulliken charges) and 2 (magnetizability and nuclear shielding).

† $\boldsymbol{m}_i = -\frac{1}{2}(\boldsymbol{l}_i + \boldsymbol{s}_i)$ where $\boldsymbol{l}$ and $\boldsymbol{s}$ are the orbital and spin angular momenta, respectively. The spin operators can be ignored for closed-shell states.

Table 1 Total energies, valence and low-lying virtual orbital energies and Mulliken charges

	VO_4^{3-}	CrO_4^{2-}	MnO_4^-
E_{SCF}	−1241.9789	−1342.5302	−1448.8691
valence orbitals			
$5t_2$	+0.0617	−0.1885	−0.4715
1e	+0.0783	−0.1622	−0.4183
$6a_1$	+0.1068	−0.0962	−0.3081
$6t_2$	+0.1269	−0.0880	−0.3308
$1t_1$	+0.1811	−0.0292	−0.2784
virtual orbitals			
dt_2	+0.2929	+0.2131	+0.1274
da_1	+0.3014	+0.2174	+0.1261
$7t_2$	+0.5002	+0.3820	+0.2009
$7a_1$	+0.5086	+0.3842	+0.2518
$8t_2$	+0.5570	+0.4390	+0.2722
2e	+0.5870	+0.4408	+0.2014
charges			
q(X)	+1.23	+0.75	+0.67
q(O)	−1.06	−0.69	−0.42

Properties are expressed in atomic units: 1 au of $E = E_h \approx 4.35975 \times 10^{-18}$ J.

Table 2 Nuclear magnetic shieldings and magnetizability

	VO_4^{3-}	CrO_4^{2-}	MnO_4^-
σ^d(X)	+1909.9	+2018.3	+2124.2
σ^p(X)	−3406.9	−8242.2	−38317.8
σ(X)	−1497.0	−6223.9	−36193.6
σ^d(O)	+614.9	+624.6	+628.0
σ^p(O)	−958.8	−1691.7	−6186.9
σ(O)	−343.9	−1067.1	−5558.9
ξ^d	−81.647	−72.413	−67.550
ξ^p	+80.810	+85.983	+160.727
ξ	−0.837	+13.570	+93.178
ξ(inner)	−12.652	−11.402	−10.507
$\xi(5t_2)$	+8.795	+19.090	+75.409
ξ(1e)	+0.671	+3.056	+16.087
$\xi(6t_2)$	−1.875	+0.561	+12.484
$\xi(6a_1)$	−2.209	−2.020	−2.473
$\xi(1t_1)$	+6.433	+4.285	+2.178

Shieldings σ are reported in ppm, and the origin of the vector potential is taken to be at the nucleus of interest in each case. For the magnetizability ξ the origin of vector potential is on the metal. The shieldings and magnetizability (in au) are listed as diamagnetic, paramagnetic and total terms. Also included is the total contribution to ξ of the inner shells and of each valence shell.

The orbital configuration in the ground state is

$$^1A_1: (1a_1)^2(2a_1)^2(1t_2)^6(3a_1)^2(2t_2)^6(4a_1)^2(3t_2)^6(5a_1)^2 (4t_2)^6(5t_2)^6(1e)^4(6a_1)^2(6t_2)^6(1t_1)^6$$

in all three cases, except that the $6a_1$ and $6t_2$ orbitals are interchanged in the order of energies in permanganate. The orbitals $1a_1$ to $2t_2$ are the atomic inner-shell orbitals 1s, 2s and 2p on the metal and 1s on the oxygens. The $4a_1$ and $3t_2$ orbitals are essentially 3s and 3p on the metal while $5a_1$ and $4t_2$ are mildly polarized oxygen 2s with small contributions from metal orbitals required to preserve orthogonality to lower-lying orbitals of the same symmetry. The valence orbitals are $5t_2$ to $1t_1$ and are constructed almost entirely of metal 3d and oxygen 2p atomic orbitals. Representative contour plots for MnO_4^- have been given in our previous work.[2] The corresponding plots for VO_4^{3-} are shown in Fig. 1, and they are qualitatively similar to those of permanganate. The $6t_2$ and $6a_1$ are weakly bonding orbitals that

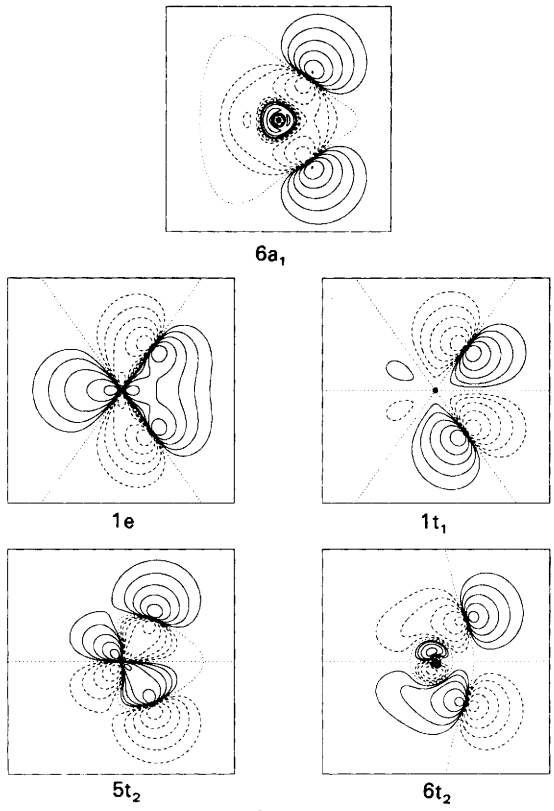

Fig. 1 Valence orbitals of VO_4^{3-} in a plane containing the V and two Os. The frame is a $16a_0$ square with centre on the V. The contour values are 0.0, $\pm 0.01 \times 2^n a_0^{-3/2}$ ($n = 0, 1, 2, \ldots$).

are essentially ligand 2p with orthogonality contributions from the metal, and $1t_1$ is non-bonding O $2p_\pi$. The principal bonding orbitals are $5t_2(\sigma)$ and $1e(\pi)$. The contour plots for these suggest that both σ and π bonds are quite strongly polarized towards the oxygens in VO_4^{3-}. The plots for MnO_4^- show strong polarization towards the metal in $5t_2$ and some polarization towards the oxygens in 1e. The orbitals in CrO_4^{2-} are intermediate in character. These observations are consistent with the view that π bonding in transition-metal complexes increases from left to right in the row. They are also supported by the Mulliken charges on the metals, given in Table 1; whilst these charges have little absolute significance, they are valuable for showing trends in related systems.

A feature of calculations in multiply charged anions is that they often give positive energies for the highest occupied orbitals. This is a consequence of the physical fact that such ions are unbound, and owe their existence to the stabilising effect of a crystal lattice or solvation cage; in Hartree–Fock theory solutions to the SCF equations exist within the constraints imposed by symmetry and a finite basis. The triply charged orthovanadate anion is a spectacular example, with five positive eigenvalues in our calculation (Table 1). Embedding the charge distribution in an appropriate lattice will change these energies to negative values, but will not change the calculated properties of the ion greatly (see Section 7). Monatomic anions are much more sensitive than are polyatomics to lattice effects.[2,34]

The virtual orbitals that are obtained as by-products of an SCF calculation, and the associated excited orbital configurations, do not have, individually, any clear physical significance. They are normally diffuse functions and, for example in a configuration interaction (CI) calculation, the whole or a large subset of the manifold of excited states is required to

give an accurate description of electron correlation or a physically significant representation of an excited state of the system. The same is true for a second-order property such as the paramagnetizability given as a sum over states [eqn. (3)]. In some cases, however, one or several of the virtual orbitals are well localized within the volume of the molecule and can be identified as the unoccupied part of a partially occupied shell. In CI calculations their presence is often associated with 'near degeneracies' (large non-dynamical correlation), whereby one or a small number of excited orbital configurations make a substantial contribution to the wavefunction. For the systems considered here, an extended valence shell can be defined which consists of all the molecular orbitals formally constructed from the O 2p and metal 3d atomic orbitals. This extended shell contains the occupied valence orbitals and the antibonding partners of the bonding orbitals 1e and $5t_2$. It was shown in our previous work[2] that two sets of virtual orbitals in MnO_4^- can be identified with these unoccupied orbitals.

As with the larger basis sets for MnO_4^- in our previous work,[2] the presence of diffuse basis functions gives rise to some very diffuse virtual orbitals with low energies. For all three ions, the lowest a_1 and t_2 orbitals have almost no density within the volume of the ion, and no physical significance. They are included in Table 1 for completeness, and denoted by da_1 and dt_2. The lowest physically significant virtual orbitals in MnO_4^- (Fig. 2 in ref. 2) are the near-degenerate 2e, the antibonding π-orbital partner of 1e, and $7t_2$, the antibonding σ-orbital partner of $5t_2$. They occupy the same volume of space as do the occupied orbitals; all other virtual orbitals listed in Table 1 are considerably more diffuse. In CrO_4^{2-}, both the virtual orbitals 2e and 3e have substantial density within the volume of the ion, with the high-energy 3e resembling more closely an anti-bonding partner of 1e. All the lowest-lying virtual t_2 orbitals are diffuse. In VO_4^{3-}, the 2e orbital is diffuse and the high-energy 3e is the antibonding partner of 2e, with all other virtual orbitals diffuse.

The results of the coupled Hartree–Fock calculations are summarized in Table 2. For the magnetizability, the diamagnetic component ξ^d shows a fairly simple size dependence. ξ^d is proportional to the moment of inertia of the electron distribution about the centre of the molecule (with our choice of origin of vector potential), and a simple point-charge model of the molecule[2] suggests an R^2 dependence for ξ^d; the computed values are roughly consistent with this but rise more steeply (more like R^3). For the large basis sets used in this work, the computed values of ξ^d are expected to be close to the Hartree–Fock limit and, as simple expectation values, can be expected to be fair estimates of the 'experimental' diamagnetizabilities of the ions. The experimental total magnetizability of MnO_4^- is $\xi = 8.34$ au, giving an 'experimental' paramagnetizability $\xi^p \approx 75.9$ au. The computed value is about twice this, giving a total magnetizability that is an order of magnitude larger than the observed value. The experimental magnetizability of CrO_4^{2-} is $\xi \approx 6.3$ au, giving an 'experimental' paramagnetizability $\xi^p(CrO_4^{2-}) \approx 78.7$ au. The computed value is *ca.* 10% bigger than this, and gives a total magnetizability that is *ca.* twice the observed value. No experimental value is available for VO_4^{3-}. However, the experimental values of ξ^p for MnO_4^- (75.9 au) and CrO_4^{2-} (78.7 au) suggest that the computed SCF value of 80.8 au is close to the true value for VO_4^{3-}. It therefore appears that there is no essential qualitative difference in the response of the three ions to an external magnetic field, the changes in magnetizability on going from VO_4^{3-} to MnO_4^- being essentially a size effect arising from the increase of nuclear charge. Hartree–Fock theory is seen to provide a satisfactory model for the magnetizability of VO_4^{3-} and CrO_4^{2-}, but to break down for MnO_4^-.

The failure of Hartree–Fock theory in describing the magnetizability of MnO_4^- has been discussed in some detail in our previous work.[2] The new calculations on VO_4^{3-} and CrO_4^{2-} confirm the conclusions of that work, and provide further insight. The orbital contributions listed in Table 2 show that the computed magnetizability in MnO_4^- is dominated by the bonding orbital $5t_2$ with significant contributions from 1e and $6t_2$, but that these are considerably reduced in CrO_4^{2-} and VO_4^{3-}. These observations can be understood in terms of the spectrum of excited orbital states. Contributions to the paramagnetizability sum-over-states [eqn. (3)] come from virtual transitions from the $^1A_1$ ground state (in T_d symmetry) to states of type $^1T_1$. In coupled Hartree–Fock theory such transitions are described by single excitations from occupied to virtual orbitals. For most molecules in closed-shell ground states, the 'normal' case, the absence of low-lying excited states results in a large number of states making small contributions to the sum-over-states. When there exist low-lying states these can make additional large contributions. This is particularly true if, as in MnO_4^-, one or more of the virtual orbitals are essentially unoccupied valence orbitals. In MnO_4^- the near-degenerate 2e and $7t_2$ are the unoccupied antibonding partners of the bonding orbitals 1e and $5t_2$, and they occupy very much the same volume of space, whilst all the other virtual orbitals are more diffuse. The first $^1T_1$ state is therefore expected to be dominated by one-electron transitions from occupied valence orbitals in the ground state to 2e ad $7t_2$. It was shown in our previous work[2] that, for the magnetizability, the relevant transitions are $5t_2, 6t_2 \rightarrow 2e$ and 1e, $1t_1 \rightarrow 7t_2$, and that the lowest $^1T_1$ state makes by far the largest contribution to ξ^p.

Within the Hartree–Fock model, there also exist low-lying $^1A_1$ states dominated by the one-electron transitions $1e \rightarrow 2e$ and $5t_2, 6t_2 \rightarrow 7t_2$, and a more accurate description of the bonding in MnO_4^-, and of the magnetizability, would be obtained from CASSCF or an equivalent CI method in which the active space includes the antibonding orbitals 2e and $7t_2$.[2,35] The inclusion of electron correlation results in both a strengthening of the covalent bonding in the molecule and in an effective increase in the energies of the manifold of excited states. Both these effects would lead to smaller contributions of the low-lying excited states to the sum.

The computed virtual orbitals in VO_4^{3-} show some important differences from those in MnO_4^-: all the low-lying t_2 orbitals are diffuse, and it is the high-energy 3e that corresponds most closely to the antibonding partner of 1e. As a result, the lowest $^1T_1$ state is not simply described in terms of a small number of one-electron transitions from the ground state, and there is no low-energy, high-overlap transition to give a very large orbital contribution to ξ^p as found in MnO_4^-. Electron correlation can be expected to decrease the magnetizability, but the absence of the 'near-degeneracy effects' found in MnO_4^- implies that correlation effects will be relatively small. CrO_4^{2-} lies between the two extremes.

It has been observed[2,35] that the SCF bond length in MnO_4^- is substantially shorter than the observed value, and[2] that the computed magnetizability is greatly reduced at the shorter distance. The SCF bond lengths computed with the present basis are $3.23a_0$ in VO_4^{3-}, $3.04a_0$ in CrO_4^{2-} and $2.92a_0$ in MnO_4^-, compared with $R_{exp} = 3.23$, 3.11, $3.08a_0$ respectively. These results support the proposition that the Hartree–Fock model provides a progressively more accurate description of the electronic structure on going from MnO_4^- to VO_4^{3-}. The corresponding computed magnetizabilities, 8.5 au in CrO_4^{2-} and 25.9 au in MnO_4^-, follow the same trend. A calculation for the experimentally unknown FeO_4, in the

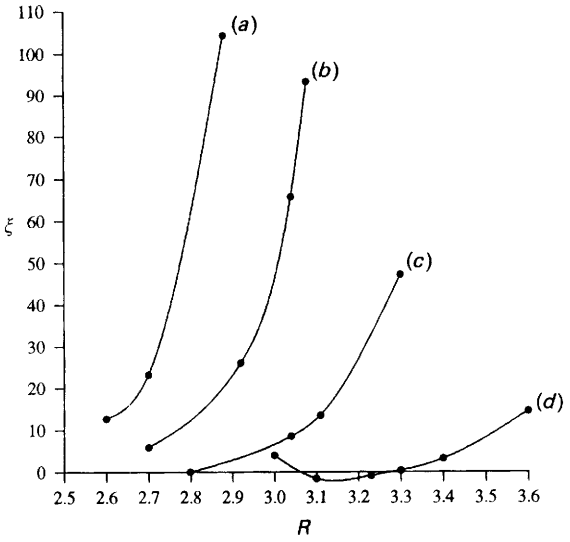

Fig. 2 Dependence of total magnetizability ξ on bond length. The quantities are in atomic units. (*a*) FeO_4, (*b*) MnO_4^-, (*c*) CrO_4^{2-} and (*d*) VO_4^{3-}.

basis set described in Section 3 gave the SCF bond length $2.88a_0$ and magnetizability +104.2 au, showing the same unrealistic behaviour found for MnO_4^- at R_{exp}.

The dependence of magnetizability on bond length is shown in Fig. 2. As discussed in our previous work[2] the behaviour in MnO_4^- at R_{exp} and beyond suggests a breakdown, in Hartree–Fock theory, of the simple model of a covalent ground state in the presence of the external magnetic field. The behaviour in CrO_4^{2-} shows little sign of breakdown at R_{exp}, whilst the magnetizability of VO_4^{3-} is close to its minimum in Hartree–Fock theory.

6. Electron Current Densities

The application of a uniform magnetic field to an electron distribution induces a diamagnetic circulation whose field opposes the external one. In a molecule the free circulation of electrons is impeded by their interaction with the nuclei and this can be described as a paramagnetic countercirculation.[1]

For a molecule in the uniform magnetic field $\boldsymbol{B}$, coupled Hartree–Fock theory gives a perturbed wavefunction in which each perturbed orbital has the form

$$\psi = \psi_0 + \mathrm{i}B_\alpha\psi_\alpha$$

where $\mathrm{i} = \sqrt{-1}$, ψ_0 is the (real) orbital in the absence of the field, and ψ_α is the (real) perturbation of the orbital (per unit field component B_α). Plots of the first-order perturbations ψ_α in MnO_4^- were given in our previous work.[2] The corresponding plots for the orbitals $5t_2$ and $1t_1$, which dominate the paramagnetism in VO_4^{3-}, are given in Fig. 3. The $5t_2$ perturbed function resembles closely, in extent and nodal structure, the virtual orbital 3e, the antibonding partner of the bonding π orbital 1e, and the paramagnetism of the orbital can be described pictorially[2] in terms of a two-centre $\sigma \rightarrow \pi$ rotation in each bond. The $1t_1$ perturbed function, on the other hand can be described as a one-centre $\pi \rightarrow \sigma$ rotation on each oxygen with charge transfer into the σ bond. The perturbed functions for the less important orbitals (insofar as the paramagnetism is concerned) show the appropriate rotations, with charge transfer from oxygen to metal for 1e and $6t_2$ but very little charge transfer for $6a_1$.

Each occupied orbital makes a diamagnetic and a paramagnetic contribution to the total electron current density; $\boldsymbol{j} = \boldsymbol{j}^{\mathrm{d}} + \boldsymbol{j}^{\mathrm{p}}$, where

$$\boldsymbol{j}^{\mathrm{d}} = \boldsymbol{A}\psi_0^2$$

$$\boldsymbol{j}^{\mathrm{p}} = B_\alpha(\psi_0 \nabla\psi_\alpha - \psi_\alpha \nabla\psi_0)$$

and $\boldsymbol{A} = \frac{1}{2}\boldsymbol{B} \times \boldsymbol{r}$, where $\boldsymbol{r}$ is the position with respect to the origin of the vector potental $\boldsymbol{A}$.

A representation of the total current density in the three ions is given in Fig. 4. In each case the plane contains the

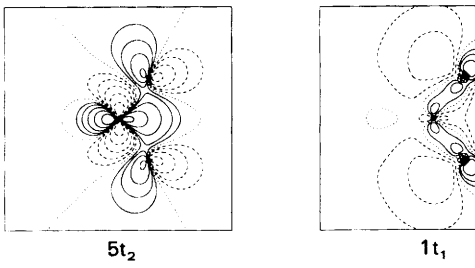

Fig. 3 Virtual orbitals in VO_4^{3-}. The frame and contour values are as in Fig. 1.

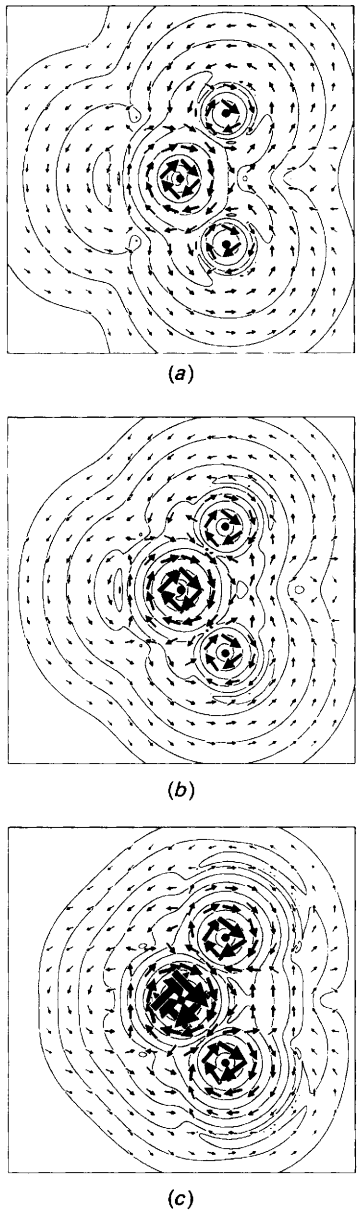

Fig. 4 Total current density. (*a*) VO_4^{3-}, (*b*) CrO_4^{2-} and (*c*) MnO_4^-. See text for description and details.

Table 3 Total and valence orbital energies, magnetizability for the ions in the model lattice (the quantities in parentheses are the changes from the values for the free ions)

	VO_4^{3-}	CrO_4^{2-}	MnO_4^-
E_{SCF}	−1244.2516 (−2.273)	−1343.5225 (−0.992)	−1449.1181 (−0.249)
$5t_2$	−0.6923 (−0.754)	−0.6784 (−0.490)	−0.7164 (−0.245)
1e	−0.6918 (−0.770)	−0.6615 (−0.499)	−0.6659 (−0.248)
$6a_1$	−0.6369 (−0.744)	−0.5735 (−0.477)	−0.5430 (−0.235)
$6t_2$	−0.6308 (−0.758)	−0.5817 (−0.494)	−0.5780 (−0.247)
$1t_1$	−0.5632 (−0.744)	−0.5224 (−0.493)	−0.5271 (−0.249)
ξ^d	−80.751 (+0.897)	−71.640 (+0.773)	−67.200 (+0.350)
ξ^p	+80.149 (−0.661)	+85.297 (−0.687)	+150.233 (−10.49)
ξ	−0.602 (+0.236)	+13.657 (+0.086)	+83.033 (−10.15)

For details and units see Tables 1 and 2.

metal and two oxygens, with unit magnetic field at right angles to the plane. The frame is a $14a_0$ square with its centre on the metal. The contours are for the modulus of total probability current density (in atomic units $\hbar/m_e a_0^4$), with values $\pm 0.0001 \times 4^n$ au ($n = 1, 2, \ldots$). The arrows give the current density vector at the mid point of each arrow, and their lengths are given by the inverse logarithmic scale $l = -a/\log(v/V)$, where v is the modulus of current density and $V = 150$ au, greater than the largest v, was chosen to give a suitable representation of the values (as was the parameter a). The logarithmic scale is necessary because of the wide range of values and the very sharp drop away from the immediate vicinity of the nuclei; the smallest arrow in each case represents current density 0.0001 au, whereas the largest arrows shown represent density 4.98 au in VO_4^{3-}, 13.4 au in CrO_4^{2-}, 62.1 au in MnO_4^-. It is seen that each nucleus is enveloped in a paramagnetic (clockwise) circulation of electrons that increases in strength and extent from VO_4^{3-} to MnO_4^-, and lies inside a general diamagnetic (anticlockwise) circulation. Considerations of the magnitudes of the diamagnetic and paramagnetic contributions to the magnetizability suggest that the computed currents in VO_4^{3-} and CrO_4^{2-} are a fair representation of the currents generated in these ions, whilst those in MnO_4^- are greatly exaggerated. The paramagnetic circulation around each nucleus enhances the magnetic field at the nucleus; there is anti-shielding of both oxygens and metal in all three ions, as shown by the computed (negative) magnetic shielding constant in Table 2. Here again, the effects in MnO_4^- are greatly exaggerated within Hartree–Fock theory.

7. Lattice Effects

A comparison of the computed magnetizability of an anion with the experimental value needs ideally to take into account not only electron correlation but also the effects of the lattice. The XO_4^{n-} ions exist in a variety of lattice structures, with local geometry and number of nearest neighbours dependent on the nature of the cations and of the phase of the solid. Anions are stabilized by their interactions with their neighbours in the lattice, and these interactions can have significant effects on electric and magnetic properties.[36]

In our previous work,[2] the electrostatic lattice effects in $KMnO_4$ were studied by replacing the real infinite lattice by a finite lattice of point charges with the experimental lattice parameters, around one MnO_4^- unit in its experimental geometry. The low local symmetry (C_s) meant that only a very low-accuracy calculation of the effect of lattice on the properties of the ion was possible. In the present work the lattice effects are studied by placing the idealised tetrahedral ion (see Section 2) at the centre of a model point-charge lattice which mimics the average electrostatic environment in the real solids. The model is a finite body-centred cubic lattice consisting of 2^3 unit cells, with the ion of interest replacing the (negative) point charge at the centre. Electrical neutrality was ensured by a suitable choice of the surface charges. The orientation of the ion within the lattice was chosen to maintain the T_d symmetry. The model describes 1 : 1 ionic solids; for example $KMnO_4$, $HgCrO_4$, $LaVO_4$. Each unit cell contains four molecules, and the lattice parameter, $a = 7$ Å for all three ions, has been chosen to give nearest-neighbour oxygen–cation distances close to those observed.

The results for the model ion in a lattice are given in Table 3. The quantities in parentheses are the changes from the free-ion values. It can be seen that all the occupied orbitals are stabilized to the same extent in each ion; $\Delta\varepsilon \approx -0.247n$ for the orbitals, $\Delta E \approx -0.247n^2$ for the total energy, where n is the magnitude of the ionic charge. The ion therefore inhabits a well of effectively constant potential created by the lattice, so that many of its properties are unchanged. Plots of the occupied orbitals show only small changes from those for the free ions. The computed diamagnetic and paramagnetic components of the magnetizability have all changed by only *ca.* 1% or less, except for ξ^p in MnO_4^- which is decreased by 7% (in contrast to the 10% increase previously obtained in a different lattice and with a very small basis[2]). At the SCF bond length in MnO_4^-, the change in ξ^p is only 1%. There are many approximations in the relatively crude simulation, but it is clear from these results that lattice effects are in all cases very small.

8. Conclusions

A consistent picture of the magnetism for a series of isoelectronic molecules is given by coupled Hartree–Fock theory. In each case the presence of low-lying empty orbitals derived from splitting of the partially occupied valence shell leads to a significant paramagnetic contribution to the total magnetizability. From MnO_4^- to VO_4^{3-}, as the central charge falls, the bonding becomes more ionic, the metal–oxygen bond grows longer and the diamagnetic susceptibility increases in magnitude. At the same time, in Hartree–Fock theory, the virtual orbitals become more diffuse and the paramagnetic contribution falls (in contrast, the experimental magnetizabilities indicate a small rise in paramagnetic contribution). As a result the anions change from being 'strongly' paramagnetic (MnO_4^-) to magnetically neutral (VO_4^{3-}).

Comparison of the computed properties with the experimental values shows that the Hartree–Fock description becomes more appropriate as the system becomes more ionic. Hartree–Fock theory gives a paramagnetic contribution to the total magnetizability of permanganate, and to a lesser extent of chromate, that is too large, but we believe that it gives an accurate description of the magnetism in the orthovanadate anion, and that it is useful across the series.

Appendix

Table A.1 Polarized (16s12p6d4f/9s7p3d2f) GTO/CGTO basis set for V

GTO	CGTO	exponent	contraction coefficients		
s subset					
1	1→3	226 090.0	0.000 253 3	−0.000 075 7	−0.000 027 3
2		33 904.48	0.001 964 2	−0.000 582 8	−0.000 211 4
3		7 719.623	0.010 173 5	−0.003 073 1	−0.001 105 5
4		2 192.247	0.040 956 9	−0.012 395 5	−0.004 524 9
5		719.366 4	0.129 766 1	−0.042 325 7	−0.015 281 9
6		262.189 5	0.302 450 5	−0.108 632 5	−0.040 772 5
7		103.695 3	0.416 431 6	−0.213 874 6	−0.080 183 5
8		43.261 27	0.231 478 8	−0.137 056 1	−0.060 902 7
9		13.492 13	0.020 027 6	0.507 687 6	0.285 970 8
10		5.569 443	−0.003 708 5	0.610 866 3	0.483 932 6
11	4	1.429 822	1.0		
12	5	0.913 846	1.0		
13	6	0.584 069	1.0		
14	7	0.091 316	1.0		
15	8	0.035 126	1.0		
16	9	0.013 512	1.0		
p subset					
1	1→2	1 397.334	0.002 140 4	−0.000 752 5	
2		331.678 1	0.017 329 9	−0.006 067 8	
3		107.075 6	0.081 214 1	−0.029 516 2	
4		40.335 35	0.241 210 4	−0.089 883 1	
5		16.475 89	0.425 895 1	−0.174 200 9	
6		7.023 516	0.357 014 7	−0.119 614 1	
7		2.755 288	0.072 988 3	0.282 929 1	
8	3	1.154 607	1.0		
9	4	0.440 538	1.0		
10	5	0.091 316	1.0		
11	6	0.035 126	1.0		
12	7	0.013 512	1.0		
d subset					
1	1	29.982 31	0.022 448 6		
2		8.300 332	0.123 661 9		
3		2.740 692	0.328 273 5		
4		0.954 833	0.474 903 4		
5	2	0.290 033	1.0		
6	3	0.088 098	1.0		
f subset					
1	1	2.740 692	0.198 292 2		
2		0.954 833	0.486 005 9		
3	2	0.290 033	0.664 293		
4		0.088 098	0.152 887		

Table A.2 Polarized (16s12p6d4f/9s7p3d2f) GTO/CGTO basis set for Cr

GTO	CGTO	exponent	contraction coefficients		
s subset					
1	1→3	235 945.9	0.000 267 5	−0.000 080 4	−0.000 029 3
2		35 354.35	0.002 073 2	−0.000 619 6	−0.000 226 9
3		8 061.089	0.010 708 0	−0.003 256 5	−0.001 182 3
4		2 295.175	0.042 795 5	−0.013 061 6	−0.004 813 8
5		756.577 2	0.134 168 9	−0.044 174 5	−0.016 100 9
6		277.079 8	0.307 825 4	−0.112 208 7	−0.042 584 0
7		110.266 0	0.413 579 2	−0.216 643 3	−0.082 081 8
8		46.355 23	0.222 831 6	−0.131 496 7	−0.059 772 7
9		14.778 08	0.018 735 7	0.513 508 6	0.295 502 0
10		6.134 996	−0.003 295 2	0.605 964 0	0.483 472 5
11	4	1.606 561	1.0		
12	5	1.022 667	1.0		
13	6	0.650 985	1.0		
14	7	0.098 113	1.0		
15	8	0.037 193	1.0		
16	9	0.014 099	1.0		

Table A.2—*continued*

GTO	CGTO	exponent	contraction coefficients	
p subset				
1	1→2	1 479.576	0.002 276 5	0.000 811 4
2		351.676 3	0.018 335 5	0.006 515 7
3		113.938 6	0.084 919 6	0.031 342 1
4		43.188 18	0.247 459 0	0.093 827 0
5		17.793 83	0.426 949 1	0.177 998 9
6		7.661 059	0.347 011 8	0.113 492 5
7		3.041 483	0.069 190 5	−0.296 443 4
8	3	1.273 891	1.0	
9	4	0.486 673	1.0	
10	5	0.098 113	1.0	
11	6	0.037 193	1.0	
12	7	0.014 099	1.0	
d subset				
1	1	33.99 943	0.022 961 5	
2		9.458 989	0.126 889 6	
3		3.141 800	0.335 339 4	
4		1.091 956	0.475 071 5	
5	2	0.332 721	1.0	
6	3	0.101 381	1.0	
f subset				
1	1	3.141 800	0.189 188 7	
2		1.091 956	0.454 628 3	
3	2	0.332 721	0.603 897	
4		0.101 381	0.142 911	

Table A.3 Polarized (16s12p6d4f/9s7p3d2f) GTO/CGTO basis set for Mn

GTO	CGTO	exponent	contraction coefficients		
s subset					
1	1→3	239 992.9	0.000 290 1	−0.000 087 8	−0.000 032 2
2		35 992.76	0.002 243 7	−0.000 675 0	−0.000 249 0
3		8 230.341	0.011 515 2	−0.003 523 6	−0.001 288 3
4		2 354.832	0.045 537 0	−0.014 015 6	−0.005 206 2
5		781.626 4	0.140 298 6	−0.046 654 2	−0.017 127 0
6		288.669 9	0.314 648 4	−0.116 632 7	−0.044 707 5
7		115.759 9	0.409 803 1	−0.219 757 6	−0.083 920 6
8		49.116 01	0.211 006 4	−0.122 932 6	−0.057 490 5
9		16.069 27	0.017 084 0	0.521 385 9	0.306 537 1
10		6.705 219	−0.002 816 2	0.599 209 9	0.479 149 0
11	4	1.777 888	1.0		
12	5	1.126 830	1.0		
13	6	0.714 187	1.0		
14	7	0.104 881	1.0		
15	8	0.039 207	1.0		
16	9	0.014 656	1.0		
p subset					
1	1→2	150 8.484	0.002 565 7	0.000 924 4	
2		359.039 2	0.020 459 4	0.007 364 7	
3		116.882 3	0.092 708 5	0.034 686 0	
4		44.663 19	0.260 554 2	0.100 454 8	
5		18.622 32	0.428 612 3	0.181 895 7	
6		8.139 494	0.327 368 1	0.100 162 1	
7		3.297 805	0.062 136 9	−0.313 421 5	
8	3	1.385 383	1.0		
9	4	0.531 322	1.0		
10	5	0.104 881	1.0		
11	6	0.039 207	1.0		
12	7	0.014 656	1.0		
d subset					
1	1	37.779 85	0.023 863 7		
2		10.545 86	0.131 732 9		
3		3.521 784	0.343 376 5		
4		1.224 193	0.474 735 4		
5	2	0.374 424	1.0		
6	3	0.114 519	1.0		

Table A.3—*continued*

GTO	CGTO	exponent	contraction coefficients
f subset			
1	1	3.521 784	0.182 973 9
2		1.224 193	0.429 068 4
3	2	0.374 424	0.547 461
4		0.114 519	0.120 857

Table A.4 Polarized (16s12p6d4f/9s7p3d2f) GTO/CGTO basis set for Fe

GTO	CGTO	exponent	contraction coefficients		
s subset					
1	1→3	256 515.5	0.000 293 5	−0.000 089 3	−0.000 033 0
2		38 743.30	0.002 254 8	−0.000 682 2	−0.000 253 6
3		8 881.224	0.011 525 2	−0.003 545 8	−0.001 306 4
4		2 548.566	0.045 490 3	−0.014 086 3	−0.005 272 7
5		846.234 1	0.140 199 3	−0.046 876 5	−0.017 343 7
6		313.063 7	0.313 613 0	−0.117 045 3	−0.045 228 7
7		125.830 3	0.409 204 3	−0.220 329 3	−0.084 857 0
8		53.483 45	0.212 324 5	−0.125 396 4	−0.059 099 5
9		17.615 18	0.017 387 1	0.520 053 0	0.309 746 4
10		7.365 366	−0.002 857 4	0.601 477 7	0.483 417 3
11	4	1.977 251	1.0		
12	5	1.250 621	1.0		
13	6	0.791 024	1.0		
14	7	0.112 837	1.0		
15	8	0.041 555	1.0		
16	9	0.015 303	1.0		
p subset					
1	1→2	1 669.494	0.002 498 9	0.000 910 8	
2		396.413 5	0.020 092 8	0.007 317 5	
3		128.766 0	0.091 807 0	0.034 756 8	
4		49.175 53	0.259 596 2	0.101 372 7	
5		20.530 67	0.428 792 0	0.184 497 4	
6		8.986 301	0.328 189 1	0.100 441 6	
7		3.644 181	0.062 462 2	−0.319 045 1	
8	3	1.528 451	1.0		
9	4	0.585 160	1.0		
10	5	0.112 837	1.0		
11	6	0.041 555	1.0		
12	7	0.015 303	1.0		
d subset					
1	1	41.341 15	0.024 901 3		
2		11.564 75	0.137 238 3		
3		3.869 601	0.350 263 1		
4		1.336 389	0.471 624 6		
5	2	0.402 610	1.0		
6	3	0.121 293	1.0		
f subset					
1	1	3.869 601	0.178 057 9		
2		1.336 389	0.407 971 6		
3	2	0.402 610	0.503 937		
4		0.121 293	0.094 708		

References

1 J. H. Van Vleck, *The Theory of Electric and Magnetic Susceptibilities*, Oxford University Press, London, 1932.
2 P. W. Fowler and E. Steiner, *J. Chem. Phys.*, 1992, **97**, 4215.
3 *Quantum Chemistry: The Challenge of Transition Metals and Coordination Chemistry*, NATO ASI series, C, vol. 176, ed. A. Veillard, Reidel, Dordrecht, 1986.
4 *The Challenge of d and f Functions*, ed. D. R. Salahub and M. C. Zerner, American Chemical Society, Washington DC, 1989.
5 B. Krebs and K. D. Hasse, *Acta Crystallogr., Sect. B*, 1976, **32**, 1334.
6 O. P. Singhal, *Proc. Phys. Soc.*, 1962, **79**, 389.
7 D. P. Raychaudhuri and P. N. Sengupta, *Indian J. Phys.*, 1936, **10**, 245; 253.
8 C. M. Nelson, G. E. Boyd and W. T. Smith, *J. Am. Chem. Soc.*, 1954, **76**, 348.
9 W. Tilk and W. Klemm, *Z. Anorg. Chem.*, 1939, **240**, 355.
10 A. Pacault and P. Souchay, *Bull. Soc. Chim. Fr.*, 1949, **16**, D377.
11 K. Venkateswarlu and K. Ramanathan, *Curr. Sci.* (*India*), 1955, **24**, 83.
12 N. Perakis and L. Capatos, *Compt. Rend.*, 1934, **198**, 1905.
13 *Magnetic Properties of Coordination and Organometallic Transition Metal Compounds*, Landolt–Börnstein, Series 2, vol. 2, ed. K. H. Hellwege and E. König, Springer-Verlag, Berlin, 1966.
14 Y. K. Syrkin and V. I. Belova, *Dokl. Akad. Nauk SSSR*, 1955, **105**, 517; as given in ref. 13.
15 C. E. Rice and W. R. Robinson, *Acta Crystallogr., Sect. B*, 1976, **32**, 2232.
16 J. A. Baglio and G. Gashurov, *Acta Crystallogr., Sect. B*, 1968, **24**, 292.
17 P. M. Touboul and P. Tolédano, *Acta Crystallogr., Sect. B*, 1980, **36**, 240.
18 J. K. Nimmo, *Acta Crystallogr., Sect. B*, 1981, **37**, 431.
19 K. Toriumi and Y. Saito, *Acta Crystallogr., Sect. B*, 1978, **34**, 3149.
20 I. D. Brown and R. Faggiani, *Acta Crystallogr., Sect. B*, 1975, **31**, 2364.
21 C. Stålhandske, *Acta Crystallogr., Sect. B*, 1978, **34**, 1968.
22 L. A. Welo, *Philos. Mag.*, 1928, **6**, 481.
23 W. Gray and J. Dakers, *Philos. Mag.*, 1931, **11**, 297.
24 M. E. Bedwell, J. F. Spencer and V. C. G. Trew, *Trans. Faraday Soc.*, 1949, **45**, 217.
25 G. J. Palenik, *Inorg. Chem.*, 1967, **6**, 503.
26 P. W. Fowler and A. J. Sadlej, to be published.
27 S. Huzinaga, *J. Chem. Phys.*, 1977, **66**, 4245, and supplementary material described therein.
28 A. J. Sadlej, *Collect. Czech. Chem. Commun.*, 1988, **53**, 1995.
29 A. J. Sadlej and M. Urban, *J. Mol. Struct.* (*Theochem*), 1991, **234**, 147.
30 A. J. Sadlej, *Theoret. Chim. Acta*, 1991, **81**, 45.
31 A. D. Buckingham, *Adv. Chem. Phys.*, 1967, **12**, 107.
32 S. I. Chan and T. P. Das, *J. Chem. Phys.*, 1962, **37**, 1527.
33 P. Lazzeretti and R. Zanasi, SYSMO package, University of Modena, Italy; P. W. Fowler and E. Steiner, University of Exeter, England.
34 P. W. Fowler and M. L. Klein, *J. Chem. Phys.*, 1986, **85**, 3913.
35 M. A. Buijse and E. J. Baerends, *J. Chem. Phys.*, 1990, **93**, 4129.
36 P. W. Fowler and P. A. Madden, *Phys. Rev. B*, 1984, **29**, 1035.

Paper 3/00259D; *Received* 15*th January*, 1993